



A narrative review of near-infrared fluorescence imaging in hepatectomy for hepatocellular carcinoma

WeiQi Zhang^{1,2#}, Zhenhua Hu^{2,3#}, Jie Tian^{2,3,4,5}, Chihua Fang¹

¹The First Department of Hepatobiliary Surgery, Zhujiang Hospital, Southern Medical University, Guangdong Provincial Clinical and Engineering Center of Digital Medicine, Guangzhou, China; ²CAS Key Laboratory of Molecular Imaging, Beijing Key Laboratory of Molecular Imaging, The State Key Laboratory of Management and Control for Complex Systems, Institute of Automation, Chinese Academy of Sciences, Beijing, China; ³University of Chinese Academy of Sciences, Beijing, China; ⁴Engineering Research Center of Molecular and Neuro Imaging of Ministry of Education, School of Life Science and Technology, Xidian University, Xi'an, China; ⁵Beijing Advanced Innovation Center for Big Data-Based Precision Medicine, School of Medicine, Beihang University, Beijing, China

Contributions: (I) Conception and design: W Zhang, Z Hu; (II) Administrative support: J Tian, C Fang; (III) Provision of study materials or patients: W Zhang; (IV) Collection and assembly of data: W Zhang; (V) Data analysis and interpretation: W Zhang; (VI) Manuscript writing: All authors; (VII) Final approval of manuscript: All authors.

[#]These authors contributed equally to this work.

Correspondence to: Zhenhua Hu, PhD; Jie Tian, PhD. CAS Key Laboratory of Molecular Imaging, Beijing Key Laboratory of Molecular Imaging, The State Key Laboratory of Management and Control for Complex Systems, Institute of Automation, Chinese Academy of Sciences, Beijing, China. Email: zhenhua.hu@ia.ac.cn; tian@ieec.org; Chihua Fang, MD. The First Department of Hepatobiliary Surgery, Zhujiang Hospital, Southern Medical University, Guangdong Provincial Clinical and Engineering Center of Digital Medicine, Guangzhou, China. Email: fangch_dr@163.com.

Abstract: Hepatectomy is a main therapeutic strategy for hepatocellular carcinoma (HCC), which requires removal of primary and disseminated tumors and maximum preservation of normal liver tissue. However, in a clinical operation, it is difficult to recognize the tumor tissue and its boundary with the naked eye and palpation, which often leads to insufficient or excessive resection. Near-infrared fluorescence (NIRF) imaging, a non-invasive, real-time, low-cost, and highly sensitive imaging technique has been extensively studied in surgical navigation. With the development of fluorescence imaging system and fluorescent probe, intraoperative tumor detection and margin definition can be achieved, making the operation more accurate. Advances in fluorescence imaging of HCC in the NIR region have focused on the traditional first NIR window (NIR-I, 700–900 nm), and have recently been extended to the second NIR window (NIR-II, 1,000–1,700 nm). Compared with NIR-I imaging, fluorescence imaging in the NIR-II exhibits great advantages, including higher spatial resolution, deeper penetration depth, and lower optical absorption and scattering from biological substrates with minimal tissue autofluorescence. There is no doubt that developing novel NIRF probes for in vivo imaging of HCC has high significance and direct impact on the field of liver surgery. In this article, the development of various NIRF probes for fluorescence image guided HCC hepatectomy is reviewed, and current challenges and potential opportunities of these imaging probes are discussed.

Keywords: Near-infrared fluorescence imaging (NIRF imaging); fluorescent probe; hepatectomy; hepatocellular carcinoma (HCC); NIR-I; NIR-II

Submitted Jul 15, 2020. Accepted for publication Dec 13, 2020.

doi: 10.21037/atm-20-5341

View this article at: <http://dx.doi.org/10.21037/atm-20-5341>

Introduction

Hepatocellular carcinoma (HCC) accounts for the majority (>80%) of primary liver cancers. Globally, HCC is ranked as the sixth most common neoplasm and the fourth most common cause of cancer-related death (1,2). HCC is the second most lethal tumor after pancreatic cancer, and the 5-year overall survival rates in the United States are only approximately 18% (3). With an age-standardized 5-year relative survival rate of 10.1%, HCC has the poorest survival among all cancers in China (4). The treatment of HCC is complicated, and hepatectomy remains the most important approach for achieving long-term survival. According to the Barcelona Clinic Liver Cancer (BCLC) staging system recommended by the European Association for the Study of Liver Disease (EASL) and American Association for the Study of Liver Disease guidelines (AASLD), the ideal candidates for hepatic resection are HCC patients with a solitary tumor at BCLC stage 0 or A, Child-Pugh classification A liver function with total bilirubin <1 mg/dL and excellent performance status, and without evidence of clinically significant portal hypertension (5,6). However, as many as 70% of these patients have tumor recurrence at 5 years (7,8). The high risk of recurrence is often interpreted as incomplete resection of the primary lesion (positive margin), and failure to remove all existing tumors in the liver at the time of resection (occult multifocality) (9). It is challenging to achieve accurate localization of HCC and complete tumor resection with maximum normal hepatic tissue preservation.

Since Weissleder *et al.* (10) put forward the concept of molecular imaging (MI) in 1999, various MI technologies have been widely developed and used to display specific targets at the tissue, cellular and subcellular levels, reflecting the changes of the molecular level *in vivo*. Near-infrared fluorescence (NIRF) imaging, in particular, has been increasingly used to understand the complexity, diversity and behavior of cancer (10). Traditional noninvasive NIRF imaging typically operates in the first near-infrared (NIR-I) region of the electromagnetic spectrum between 700 and 900 nm (11). Compared with visible light between 400 and 700 nm, NIR-I imaging can penetrate deeper tissues to a depth of a millimeter or even a centimeter, and maximize the signal-to-background ratio (SBR) by NIR-I fluorescent probes (12,13). Over the last decade, the invisible NIR-I fluorescence has been studied to the real-time visualization of HCC, providing a new solution for intraoperative navigation (14,15). Regarding selection

of light wavelengths, the NIR window between 1,000 and 1,700 nm, commonly known as the second near-infrared (NIR-II) window, has recently emerged as a better choice in contrast to conventional NIR-I light, because of its advantages in penetration depth, spatial resolution, tissue autofluorescence and other key indicators (11,16). With several NIR-II probes demonstrating superior performance to the clinically approved NIR-I agents, NIR-II imaging is expected to provide great help for surgeons to carry out accurate hepatic resection, and improve the postoperative survival of HCC patients. In this review, we attempt to summarize the recent advances of various NIR-I and NIR-II fluorescent probes in preclinical studies and clinical applications in hepatectomy for HCCs, and discuss the challenges and perspectives of these probes for liver surgery in the near future. We present the following article in accordance with the Narrative Review reporting checklist (available at <http://dx.doi.org/10.21037/atm-20-5341>).

NIR-I fluorescence imaging

NIR-I fluorescent probe for clinical applications

Indocyanine green (ICG)

ICG is an NIRF agent approved by the Food and Drug Administration (FDA) and the European Medicines Agency (EMA), which is suitable for human intravenous administration. It was proposed in the 1970s that protein binding ICG can be activated by extraneous light with a wavelength of 750–810 nm and emits NIR light with a wavelength of about 840 nm (17). Since ICG fluorescence imaging was first reported by Aoki *et al.* (18) to identify segments and subsegments for anatomical hepatic resection in 2008, a variety of clinical applications of ICG NIRF imaging in HCC surgery have been gradually developed.

As a non-specific fluorescent probe, ICG can be rapidly taken in by hepatic cells and excreted through the biliary system. Due to the damage of bile excretion function of hepatocytes in HCC tissue, ICG remains in the cytoplasm and/or pseudo glands for several weeks after intravenous injection, which displays fluorescence of tumoral tissues under intraoperative irradiation of exciting light (19). Tumor fluorescence enhancement realizes an initial identification of HCCs, and helps surgeons to accurately locate and demarcate the superficial, micro and satellite foci under laparotomy and laparoscopy. The phenomenon of ICG aggregation in HCC tissue was accidentally found in 2007. Ishizawa *et al.* (15) carried out a prospective study

aiming to demonstrate clear visualization of HCC, and they reported the results for the first time in 2009. ICG fluorescence imaging identified all 63 HCCs confirmed by postoperative pathology, and 8 of 63 HCCs that were missed by preoperative examinations were detected by ICG NIRF. Gotoh *et al.* (20) collected 10 cases with solitary HCC at about the same time, and they found 4 new HCC nodules that only ICG NIRF imaging could detect. All of the newly detected HCC nodules were very small in size (<6 mm in diameter) and most of the tumors were well-differentiated HCCs. Except for intrahepatic HCC, Satou *et al.* (21) reported in 2013 that extrahepatic lesions including the peritoneum, lymph nodes, lungs, and adrenal glands exhibited ICG fluorescence and were confirmed to be HCC metastases pathologically. In the same year, Morita *et al.* (22) preliminarily discussed whether ICG fluorescence can improve the prognosis of patients with HCCs. Through the follow-up of 58 HCC patients who received intraoperative ICG fluorescence guided resection, the short-term postoperative recurrence of these patients within 12 months tended to be diminished compared with the control group. Further research in 2014 by Ishizawa *et al.* (19) revealed that 273 out of 276 HCCs were identified by ICG fluorescence imaging with a sensitivity of 99%. Besides, they also found that the HCCs with low differentiation showed a ring fluorescence pattern, but HCCs with high and medium differentiation had a full and partial fluorescence pattern, respectively. Kudo *et al.* (23) then developed laparoscopic ICG NIRF imaging technology and evaluated the effect of identifying subcapsular HCCs, which made up for the shortage of palpation in laparoscopic hepatectomy. Recently, Zhang *et al.* (24) demonstrated the high potential of intraoperative ICG NIRF detection for small and grossly unidentifiable HCCs, and the smallest HCC nodule they detected was approximately 2 mm in diameter.

Since Makuuchi *et al.* (25) reported anatomical hepatectomy in 1985, this surgical approach has played an important role in the treatment of HCC. In 2008, Aoki *et al.* (18) first reported a highly sensitive ICG fluorescence imaging technique for identifying hepatic segments and subsegments in anatomic hepatectomy. Out of 35 patients with malignant liver tumors, stained liver subsegments and segments of 33 cases were recognized. Their further study, reported in 2010, proved that this method can clearly delineate the hepatic segments even in the background of cirrhosis (26). This fluorescent staining technique is simple for open surgery; however, it is much more difficult to reproduce these procedures laparoscopically. In 2012,

Ishizawa *et al.* (27) developed a laparoscopic ICG NIRF imaging system, and they applied the system to the positive-staining technique by laparoscopic ultrasound-guided puncture of segment IV portal vein for ICG injection and a negative-staining technique by segment III portal pedicle clamping and peripheral vein ICG injection. In 2015, Inoue *et al.* (28) described their initial experience of fusion ICG NIRF imaging applied to anatomical hepatectomy with three-dimensional identification of liver territories. With this method, they safely obtained more accurate and clearer anatomical resection navigation than conventional ICG NIRF imaging. Compared with the previously reported higher dose of ICG injection (18,28), Miyata *et al.* (29) modified the hepatic staining technique based on the injection of an indigo-carmin solution spiked with a small amount of ICG (0.25 mg) into the portal branch, especially for patients whose liver was covered by connective tissue from previous operations. In 2017, the technical details of five types of fluorescence staining techniques including single staining, multiple staining, counterstaining, negative staining, and paradoxical negative staining were demonstrated by Kobayashi *et al.* (30). These techniques have been proved to be safe and facilitate real-time and clear visualization of the portal vein territory, enhancing the efficacy of anatomical resection of such territories. In recent years, there were a growing number of case reports concerning anatomical laparoscopic segmentectomy using a positive or negative staining method with ICG NIRF imaging (31-35). On the basis of advanced laparoscopic skills, the role of ICG fluorescent visualization of hepatic segmental boundaries has been emphasized to assist in these technically challenging operations.

At present, the application of ICG fluorescence imaging in hepatectomy for HCCs remains to suffer two major limitations. One is the limited tissue penetration depth. It has been reported that tumors located deeper than 10 mm from the liver surface are difficult to identify as luminous nodules, presumably, their maximum detection depth is only 10 mm (36). The other limitation is the high false-positive detection rate of HCC nodules. ICG fluorescence is also shown in benign lesions such as regenerative nodules and cirrhosis, resulting in a false positive rate of 40–50% (20).

5-aminolevulinic acid (5-ALA)

5-ALA is the main substrate for the synthesis of protoporphyrin, which has been used clinically for tumor fluorescence imaging and photodynamic therapy. In cancer cells, 5-ALA causes intracellular synthesis and accumulation

of protoporphyrin IX (PpIX). There are two main fluorescence emission peaks in PpIX with approximately half of their fluorescence emission centered at ~700 nm (37). In 2002, Schneider *et al.* (38) presented the first experience of 5-ALA fluorescence-based diagnostic laparoscopy in a patient with HCC. Fluorescence laparoscopy revealed several small metastases of HCC, which were ignored under the traditional white-light illumination. Inoue *et al.* (39) used 5-ALA in 2014 for the diagnostic and surgical procedures of malignant liver tumor demarcation via fluorescence guidance. Their study showed that 5-ALA fluorescence was detected in all 24 HCCs with serous infiltration, providing a higher sensitivity than the traditional white light real-time irradiation. In 2016, Kaibori *et al.* (40) compared ICG and 5-ALA in intraoperative fluorescein imaging for detecting superficial liver tumors. The sensitivity, specificity, and accuracy of 5-ALA and ICG for detecting preoperatively identified main tumors were 57% and 96%, 100% and 50%, and 58% and 94%, respectively. 5-ALA fluorescence imaging may provide higher specificity and lower sensitivity than using ICG fluorescence imaging alone in the detection of surface-invisible malignant liver tumors. Because hypotension and alteration of liver functions have been reported as potential adverse effects of oral 5-ALA (41), the main advantages of ICG over 5-ALA are its safety and commercial availability.

NIR-I fluorescent probe for preclinical studies

NIR-I fluorescent probe

The construction of a novel NIRF probe requires a variety of components, and the safety of each component needs to be considered. Because of the need to evaluate from the perspective of effectiveness, safety and ethics, it takes a long time for the newly developed NIRF probe to enter clinical practice. Most of the NIR-I fluorescence probes for HCC imaging are still in the preclinical research stage (42).

In this article, the reported NIR-I fluorescent probes designed for HCC imaging and their imaging characteristics are summarized in *Table 1*. These probes are mainly active targeting probes, which are the molecules constructed by ligands or antibodies conjugated with fluorescent reporters. As mentioned above, ICG has some limitations in HCC diagnosis because of the deficiency of targeting ability. In order to improve the detection specificity and sensitivity, it is urgently needed to find a cancer-specific biomarker and its ligand, but there is still limited knowledge of suitable biomarkers for HCC. In 2011, Li *et al.* (43) first

demonstrated that sperm protein 17 (Sp17) is overexpressed on the surface of the HCC cell line SMMC-7721, and anti-Sp17 monoclonal antibody (mAb) conjugated with ICG could serve for HCC imaging *in vivo*. Lv *et al.* (44) reported an NIR-I fluorescent probe in 2013 known as lactose substituted zinc phthalocyanine. Because of the endocytosis mediated by the lactose receptor, it showed fluorescence imaging specifically targeted HCC, but not lung cancer or melanoma. Cluster of differentiation 24 (CD24) is known to be overexpressed in a variety of human tumors including HCC. In 2015, He *et al.* (45) conjugated CD24 targeted antibodies G7mAb and G7S with an NIRF dye multiplex probe amplification, and specific NIRF imaging was observed in Huh7 HCC xenograft tissue. The studies carried out by Zhu *et al.* and Qin *et al.* focused on glypican-3 (GPC3), a promising HCC-specific target as its expression was significantly elevated in HCC, but not in cholangiocarcinoma or normal liver tissue or in serum (46,47). In these two studies, phage display screening technology was used to obtain GPC3 binding peptides (GBP), and HCC tissue was successfully differentiated from normal liver tissue after intravenous injection of NIR dye Cy5.5-labeled GBP into the HepG2 HCC tumor-bearing mouse model. In 2016, Zeng *et al.* (48) synthesized arginine-glycine-aspartic acid (RGD)-conjugated highly loaded ICG mesoporous silica (ICG/MSNs-RGD) nanoparticles (NPs) as a fluorescent probe to overcome the difficulties in the highly sensitive detection of HCC microfoci. By targeting the tumor marker integrin $\alpha v \beta 3$ receptor with RGD peptide, they accurately delineated HCC margins, and the average size of the detected microtumor lesions was 0.4 ± 0.21 mm with excellent tumor-to-background ratio (TBR) of 4.7 ± 0.21 . Li *et al.* (49) emphasized the value of Cy5.5-labeled peptide specific for epidermal growth factor receptor (EGFR) in minimally-invasive surgery of HCC. A compact imaging module was attached to the proximal end of a medical laparoscope, and this integrated imaging methodology measured a mean TBR of 2.99 ± 0.22 from 13 surgically exposed subcutaneous SK-Hep1 human HCC tumors *in vivo* in 5 mice. Recently, high expression of histone deacetylases, especially HDAC6, has been found in tumor samples of HCC patients, and some HDAC inhibitors, including the FDA approved suberoylanilide hydroxamic acid (SAHA), which have strong antitumor effects on HCC (51). In 2020, Tang *et al.* (51) reported that IRDye800CW labeled SAHA (IRDye800CW-SAHA) showed rapid tumor accumulation with high TBR in both subcutaneous and orthotopic HCC mouse tumor models,

Table 1 Preclinical studies of NIR-I fluorescent probes for HCC

References, year	Imaging systems	Fluorophore	Absorption/emission wavelength	Targets	Cell lines	Maximum SBR of NIRF, Post-injection time	Margin detection information	Minimal tumor imaging
Li <i>et al.</i> (43), 2011	Self-built NIRF Imaging System	ICG-Der-02	780/835 nm	Sp17	SMMC-7721	N/A, 24 h	NMTP	N/A
Lv <i>et al.</i> (44), 2013	<i>In Vivo</i> Imaging System (Kodak FX Pro)	Zinc phthalocyanine	618/690 nm	Lactose receptor	HepG2	N/A, N/A	NMTP	N/A
He <i>et al.</i> (45), 2015	Self-built NIRF Imaging System	MPA	N/A	CD24	HuH7	2.23 ST (G7mAb), 4 h; 2.80 ST (G7S), 4 h	NMTP	N/A
Zhu <i>et al.</i> (46), 2016	<i>In Vivo</i> Imaging System (Carestream FX Pro)	Cy5.5	670/690 nm	GPC3	HepG2	3.98±0.36 ST , 4 h	NMTP	N/A
Qin <i>et al.</i> (47), 2017	<i>In Vivo</i> Imaging System (Carestream FX Pro)	Cy5.5	670/690 nm	GPC3	HepG2	6.49±0.55 ST , 4 h	NMTP	N/A
Zeng <i>et al.</i> (48), 2016	IVIS Spectrum Imaging System (PerkinElmer)	ICG	770/837 nm	Integrin $\alpha_v\beta_3$ receptor	Hep-G2	4.92±0.2 ST , 48 h	NMTP	0.4±0.21 mm ^{OT}
Li <i>et al.</i> (49), 2016	Self-built Laparoscopic NIRF Imaging System	Cy5.5	660/710 nm	EGFR	SK-Hep1	2.53±0.20 ST , 6 h	NMTP	N/A
An <i>et al.</i> (50), 2017	Lumina II Small Animal Optical Imaging System (Caliper Life Sciences)	DZ-1	767/798 nm	Nonspecific	Hep3B, SMMC-7721, C90706	N/A	NMTP	N/A
Tang <i>et al.</i> (51), 2020	IVIS Spectrum Imaging System (PerkinElmer)	IRDye800CW	775/801 nm	HDAC	Bel-7402	3.35 ST , 12 h	NMTP	N/A
Liu <i>et al.</i> (52), 2019	N/A	ABTT-NH ₂	405/680 nm	GGT	HepG2	N/A, 1h	NMTP	N/A
Wu <i>et al.</i> (53), 2020	IVIS Spectrum Imaging System (PerkinElmer)	NIR775	580/780 nm	β -Gal receptor	HepG2	71.9±8.8 ST , 12 h; 124.5±12.5 ^{OT} , 12 h	NMTP	~2.8×2.9 mm ^{2ST}

N/A, not available; ST, subcutaneous tumor; OT, orthotopic tumor; NMTP, negative margin targeting probe; HCC, hepatocellular carcinoma; NIR, near-infrared; NIRF, near-infrared fluorescence.

and the resection of orthotopic HCC was successfully guided under IRDye800CW-SAHA NIRF imaging. Another new biomarker, γ -glutamyl transpeptidase (GGT) has been reported to be of great benefit for early detection as well as intraoperative navigation of HCC. Liu *et al.* (52) designed and synthesized a novel NIRF probe, namely ABTT-Glu, coupling aggregation-induced emission and excited-state intramolecular proton transfer effect for GGT detection. The probe had almost no fluorescence in an aqueous solution; however, GGT mediated enzymatic reaction changed the aggregation state of the probe, formed an intramolecular hydrogen bond, and enhanced fluorescence emission to identify HCC with high GGT expression from normal cells. In 2020, Wu *et al.* (53) constructed an afterglow luminescent probe with high SBR. They optimized an organic π -electron structure-based

electrochromic material (EM 1²⁺) and integrated it into NIR photosensitizers {poly[2methoxy-5-(2-ethylhexyloxy)-1,4-phenylenevinylene] and silicon 2,3-naphthalocyanine bis(trihexylsilyloxy)} containing NPs to develop an H₂S-activatable NIR afterglow probe (F1²⁺-ANP). Furthermore, by incorporating β -galactose ligands on the surface, the probe realized sensitive detection of subcutaneous and orthotopic HepG2 HCC tumors *in vivo*, reaching the average afterglow SBR of 71.9±8.8 and 124.5±12.5, respectively (Figure 1).

Except for the targeting probe, heptamethine carbocyanine dye (DZ-1) was reported to recognize HCC cells directly without chemical modification. Unlike the mechanism of action of ICG, tumor hypoxia and the activation of a group of organic anion-transporting peptide (OATP) genes mediate DZ-1 uptake in HCC. Using

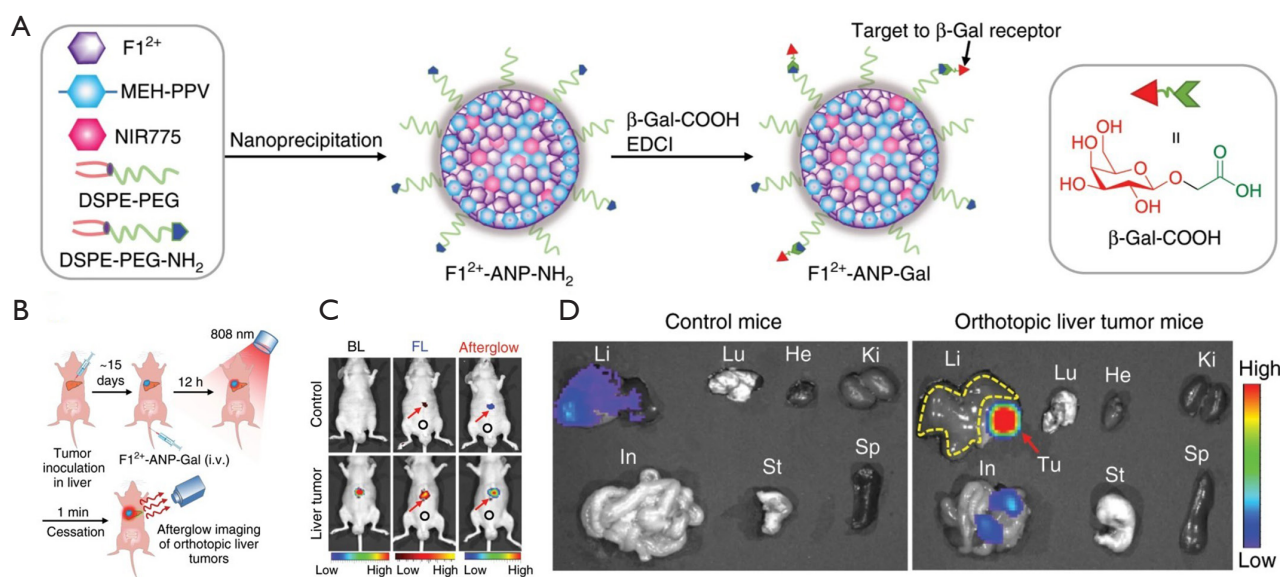


Figure 1 H₂S-activatable NIR afterglow luminescent probe for HCC imaging (53). (A) Schematic for the preparation of $F1^{2+}$ -ANP-Gal. (B) Schematic for afterglow imaging of orthotopic HepG2 tumors in living mice. (C) Bioluminescence (BL), fluorescence, and afterglow imaging of control mice and orthotopic HepG2 tumor-bearing mice at 12 h post I.V. injection of $F1^{2+}$ -ANP-Gal. (D) Representative ex vivo afterglow images of main organs resected from control mice and orthotopic HepG2 tumor-bearing mice at 12 h post I.V. injection of $F1^{2+}$ -ANP-Gal. Copyright 2020, Springer Nature. HCC, hepatocellular carcinoma.

preclinical models, cell lines, and clinical samples, DZ-1 was proved to be an effective molecular probe for tumor-specific imaging in HCC (50).

Hybrid NIR fluorescent probe

Up to now, a single imaging modality of NIRF has not been able to simultaneously provide the preoperative structural information and the intraoperative local functional information for HCC required in clinical practice. There are diverse imaging modalities of HCC, such as positron emission tomography-computed tomography (PET-CT), CT, and magnetic resonance imaging (MRI), each of which owns its pros and cons for various physiological parameters. Hybrid MI probes may have the potential to combine the advantages of two imaging techniques. Intraoperative NIRF imaging has been developed in combination with other modalities in several studies because of its high sensitivity and real-time performance, which is expected to provide more accurate detection and resection of HCC. The summary of the preclinical studies of hybrid NIRF probes for HCC are shown in *Table 2*.

Owing to excellent soft tissue contrast and spatial resolution of MRI, NIRF and MRI dual-modal probes account for the majority of the reported hybrid probes.

In general, T1-weighted contrast agents of MRI are paramagnetic lanthanide compounds, such as gadolinium (Gd^{3+}) and manganese (Mn^{2+}) chelates, while T2 weighted contrast agents are superparamagnetic, like iron oxide NPs (64). In a preliminary study reported in 2012, iron oxide NPs were covalently conjugated to Alexa Fluor 647. Human HCC cells were treated with biotin-conjugated GPC3 mAb (α GPC3), and then targeted with NPs through non-covalent streptavidin-biotin interaction. Based on the flow cytometry and MRI experiments, the α GPC3-NPs conjugate showed 4-fold mean fluorescence and 3-fold R2 relaxivity over non-targeted NPs, respectively (54). Another study showed that the “core-shell” combination of iron oxide NPs and Gd complex, and NIRF dye Cy5-labeled hybrid probe realized simultaneous dual-modal T1 and T2-weighted MRI and NIRF imaging of hepatic tumor detection in mice (55). Moreover, the probe (SPIO@Liposome-ICG-RGD) reported by Chen *et al.* (57), comprised of superparamagnetic iron oxide NPs coated with liposomes to RGD and ICG. After the probe injection in mouse models with both orthotopic liver tumors and intrahepatic tumor metastasis, preoperative MRI detected small tumors (0.9 ± 0.5 mm) with the contrast-to-noise ratio of 31.9 ± 25.4 , and intraoperative fluorescent images

Table 2 Preclinical studies of hybrid NIR fluorescent probes for HCC

References, year	Imaging modalities	Imaging systems of NIRF	Materials	Targets	Maximum SBR of NIRF, post-injection time	Margin detection information	Cell lines
Park <i>et al.</i> (54), 2011	NIRF/MRI	N/A	Alexa Fluor 647/ Iron oxide NPs	GPC3	N/A, N/A	NMTP	HepG2
Liu <i>et al.</i> (55), 2015	NIRF/MRI	N/A	Cy5/Au-Fe ₃ O ₄ NPs	Folate receptor	N/A, N/A	NMTP	Bel7402
Hernandez <i>et al.</i> (56), 2016	NIRF/PET	IVIS Spectrum Imaging System (PerkinElmer)	ZW800-1/ ⁸⁹ Zr	CD146	N/A, N/A	NMTP	HepG2, Huh7
Chen <i>et al.</i> (57), 2017	NIRF/MRI	IVIS Spectrum Imaging System (PerkinElmer)	ICG/SPIO NPs	Integrin $\alpha_v\beta_3$ receptor	2.6±0.1 ST , 72 h	NMTP	HepG2
Guan <i>et al.</i> (58), 2017	NIRF/PAT	IVIS Spectrum Imaging System (PerkinElmer)	ICG/AuNR	Nonspecific	N/A	NMTP	HepG2, Huh7
Yan <i>et al.</i> (59), 2018	NIRF/MRI	Kodak's In Vivo Optical Imaging System	IR783/Gd ³⁺ -DTPA	CD105	2.7 ^{OT} , 24h	NMTP	SMMC-7721
Jin <i>et al.</i> (60), 2018	NIRF/MRI	IVIS Spectrum Imaging System (PerkinElmer)	IRDye800 CW/ Gd ³⁺ -DOTA	GRP78	3.08±0.20 ST (HepG2), 48 h; 3.20±0.30 ST (Hep3B), 48 h; 2.06±0.11 ST (SMMC-7721), 12 h; 3.96±0.15 ST (Bel-7402), 48 h	NMTP	HepG2, Hep3B, SMMC-7721, Bel-7402
Zhang <i>et al.</i> (61), 2018	NIRF/PET	N/A	MHI-148/ ⁶⁸ Ga	Nonspecific	N/A, N/A	NMTP	Hep3B-3.1
Ai <i>et al.</i> (62), 2018	NIRF/CT	IVIS Spectrum Imaging System (PerkinElmer)	ZnGa ₂ O ₄ Cr _{0.004}	Nonspecific	5.22±0.88 ^{OT} , 6 h	PMTP	HepG2, Huh7
Shuai <i>et al.</i> (63), 2020	NIRF/CT	IVIS Spectrum Imaging System (PerkinElmer)	CNCI-1	Nonspecific	N/A, N/A	NMTP	HepG2, LM3

N/A, not available; ST, subcutaneous tumor; OT, orthotopic tumor; NMTP, negative margin targeting probe; PMTP, positive margin targeting probe; HCC, hepatocellular carcinoma; NIR, near-infrared; NIRF, near-infrared fluorescence.

captured miniscule tumor lesions (0.6±0.3 mm) with a TBR of 2.5±0.3. Because the non-specificity and transient circulation lifetime of the commercial MRI contrast agent Gd³⁺-DTPA limits its ability to detect HCC, Yan *et al.* (59) screened a new aptamer with high endothelin binding activity. By combining the aptamer with the paramagnetic agent Gd³⁺-DTPA and NIR fluorophore IR783 on the G5 dendrimer, a targeted nanoprobe was constructed. The orthotopic xenograft HCC with a diameter as low as 4 mm was successfully imaged. Jin *et al.* (60) selected the HCC targeting peptide SP94 to conjugate with an NIR dye IRDye800 CW and Gd chelated DOTA to enhance the specificity of different imaging modalities. Significant enhancement of the MRI signal in HCC was noted, and microprimary malignancy and micrometastasis foci with a diameter less than 1 mm were easily detected by NIRF

imaging after abdominal exposure in mice.

X-ray CT, like MRI, has high spatial resolution, which is the main noninvasive imaging technique to distinguish HCC from normal tissue (65). In 2018, Ai *et al.* (62) reported that ZnGa₂O₄Cr_{0.004} (ZGC), an NIR-emitting persistent luminescent NP, accurately delineated HCC in mice and supplied preoperative CT imaging. Interestingly, ZGC was found to mainly accumulate in normal liver tissue, and reverse imaging in the tumor region was observed. In 2020, Shuai *et al.* (63) conducted the first study to enhance hepatoma-specific dual-modal imaging using small molecules. The molecule CNCI-1 was synthesized by an ICG derivative and two diatrizoic acids with high liver specificity and effective CT/NIRF imaging functions. CNCI-1 was successfully applied to NIRF imaging *in vivo* in a HepG2 tumor-xenografted mouse model and LM3

Table 3 Studies of NIR-II fluorescent probes for HCC

References, year	Imaging modalities	Imaging systems of NIRF	Materials	Maximum SBR of NIRF, post-injection time	Margin detection information	Cell lines
Hu <i>et al.</i> (68), 2020	NIRF	Self-built Integrated Visible and NIR-I/II ICG Multispectral Imaging Instrument		2.25±0.06 ST (Mice), N/A; 2.43±1.16 (Patients), N/A	NMTP	HepG2
Ding <i>et al.</i> (69), 2018	NIRF	Series III 900/1700 Equipment (NIR-Optics Technologies Co.)	SCH4	7.2 ST , 1 h	NMTP	HepG2
Ren <i>et al.</i> (70), 2020	NIRF/MRI	Self-built NIRF Imaging System	NaGdF ₄ :Nd5% [@] NaGdF ₄ @Lips	2.1±0.83 ^{OT} , N/A	PMTP	HCC patient specimen

N/A, not available; ST, subcutaneous tumor; OT, orthotopic tumor; NMTP, negative margin targeting probe; PMTP, positive margin targeting probe; HCC, hepatocellular carcinoma; NIR, near-infrared; NIRF, near-infrared fluorescence.

orthotopic hepatoma mouse model, and enhanced tumor imaging by revealing the blood vessels nearby for the CT image acquisition in the VX2 orthotopic hepatoma rabbit model.

At present, the diagnosis of early HCC mainly depends on morphological features of the tumor detected by CT, MRI or contrast-enhanced ultrasound. However, these features are rarely seen in the initial stage of HCC or are not sensitive to biological changes occurring shortly after treatment (66). PET, a typical example of a functional imaging technique, is superior for noninvasive detection of tumor metabolism, tumor-associated biomarkers, and molecular pathways. Hernandez *et al.* (56) described the generation of a CD146-targeting probe via labeling of anti-CD146 mAb with the positron emitter ⁸⁹Zr, the NIRF dye ZW800-1 for dual-modal PET, and optical imaging of HCC in a mouse model. Since a previous study reported that NIRF heptachlor cyanine dye MHI-148 accumulates specifically in HCC cells (50), Zhang *et al.* (61) reported the synthesis and characteristics of the PET/NIRF optical imaging probe by using MHI-148 and ⁶⁸Ga, and its feasibility was verified in orthotopic xenotransplantation of HCC in nude mice and rabbits.

Photoacoustic tomography (PAT) has the characteristics of high spatial resolution and penetration depth (up to 7 cm). It overcomes the high degree of scattering of optical photons in biological tissue by making use of the photoacoustic effect (67). In 2017, Guan *et al.* (58) prepared ICG loaded gold nanorod@liposome core-shell NPs (Au@liposome-ICG) to integrate both imaging modalities. Preoperative PAT and intraoperative NIRF imaging confirmed the effectiveness of the dual-mode probe in detecting tumors and guiding operations in the orthotopic HCC mouse model.

NIR-II fluorescence imaging

NIR-II fluorescent probe for clinical applications

The studies of NIR-II fluorescent probes for HCC are described in *Table 3*. The development of NIR-II fluorophores and molecular probes represents an important, newly emerging and dynamic field in MI. Because of diminished tissue autofluorescence, reduced photon scattering, and low levels of photon absorption at longer wavelengths, the imaging performance of NIR-II fluorescence is better than that of visible light and NIR-I fluorescence, and latest optical imaging research indicates that NIR-II fluorescence can obviously improve tumor imaging *in vivo* (16,71). Nevertheless, due to the lack of suitable imaging instruments and optical probes, NIR-II fluorescence imaging has not been tested in clinical practice. ICG has recently been found to display tail fluorescence in the NIR-II window and has been proved to be suitable for NIR-II imaging in small animal models (72,73). Hu *et al.* (68) developed an integrated visible and NIR-I/II multispectral imaging instrument and characterized the imaging performance in human and animal research under different infrared windows (*Figure 2*). In addition, the first-in-human study of visible light, NIR-I and NIR-II multispectral imaging was carried out in 23 patients with liver tumors after ICG injection. For all the HCC patients (n=11), NIR-II imaging achieved a significantly higher tumor-to-normal tissue ratio (TNR) over NIR-I imaging (2.43±1.16 versus 1.17±0.13, P=0.024), and NIR-II imaging showed higher sensitivity and positive predictive value than NIR-I. It is worth noting that NIR-I imaging needs to turn off the light, while NIR-II imaging does not. NIR-II imaging is compatible to the lighting environment of the operating room, providing convenience and feasibility for

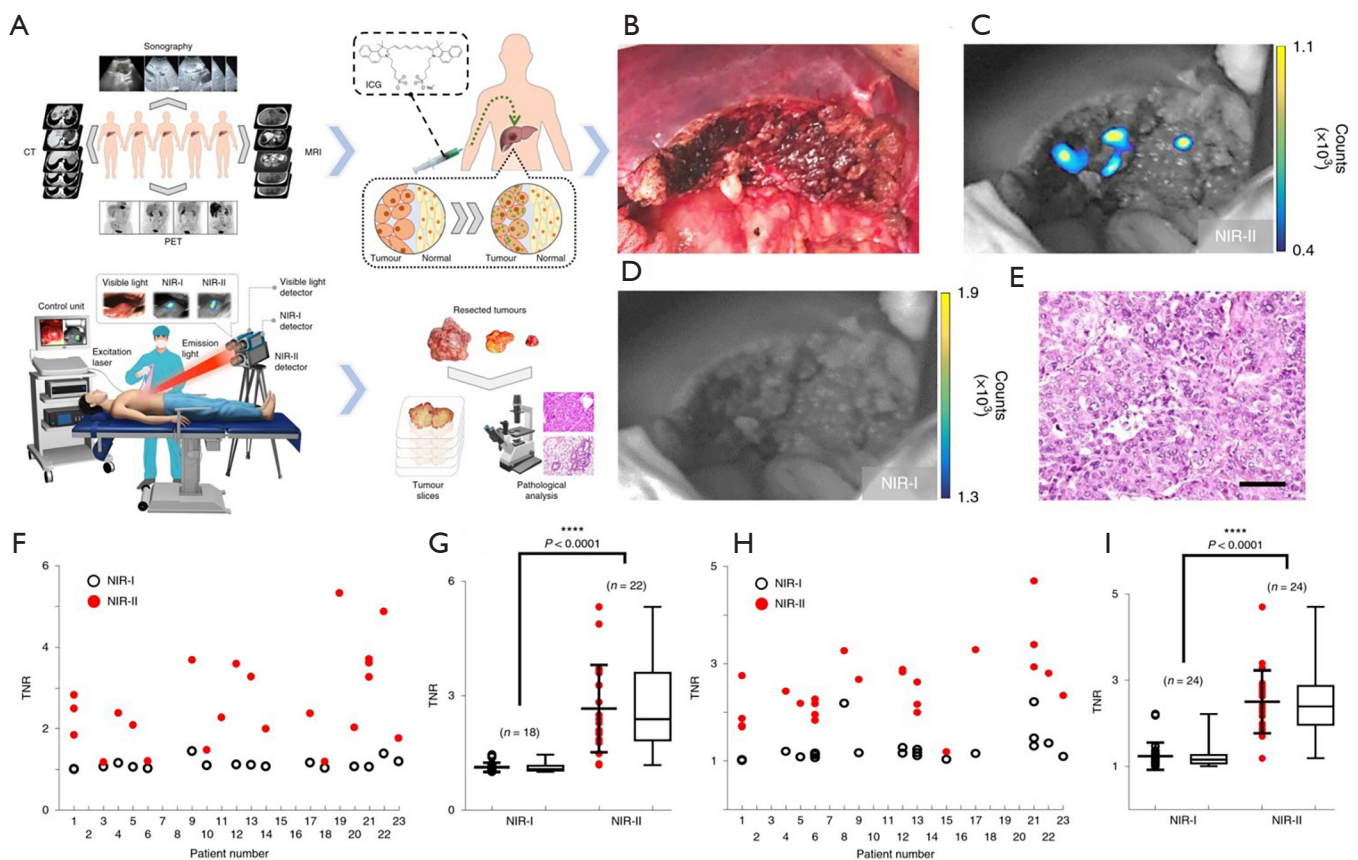


Figure 2 The visible and NIR-I/II multispectral imaging of HCC (68). (A) Schematic for description of the study plan. (B) The HCC was resected guided by ultrasonography and the visible light image and it was thought to be completely removed on the basis of the experience of the surgeons. (C) NIR-II imaging detected fluorescence signals in the remaining tissue sections. (D) NIR-I imaging did not reveal any signal. (E) The fluorescent residual tissues were further resected and received histopathological examination to verify that the tissues were HCC. (F,G) Quantitative analysis of the TNR of NIR-II and NIR-I imaging in the *in vivo* experiment, and there was a significant correlation difference between the TNR of NIR-II and NIR-I ($P < 0.0001$). (H,I) Quantification analysis of the TNR of NIR-II and NIR-I imaging in the *ex vivo* experiment, and the TNR of NIR-II imaging was significantly higher than that of NIR-I imaging ($P < 0.0001$). Copyright 2019, Springer Nature. HCC, hepatocellular carcinoma; NIR, near-infrared; TNR, tumor-to-normal tissue ratio. ****, $P < 0.0001$. (A,E) The staining method is H&E staining, and the scale bar is 50 μm .

clinical application.

NIR-II Fluorescent probe for preclinical studies

In 2016, researchers developed a novel NIR-II fluorescent molecule CH1055 (74). Its optical properties are excellent with the excitation wavelength of 750 nm and the emission wavelength of 1,055 nm. The fluorescent molecule has good biocompatibility, high stability, and *in vivo* performance, and the metabolites can be excreted through urine. Ding *et al.* (69) developed an ingenious PEGylation strategy for regulating the assembly of CH1055-based NIR-II probes

from a single molecule to NP size. By coupling CH1055 with a series of PEG short chains, a class of NIR-II probes (SCH1-SCH4) were constructed. SCH4 displayed the properties of a single molecule probe with a molecular mass of 6.7 kDa. It showed fast and high passive HCC uptake with a superior TNR (>7) in a mouse model, which was capable of facilitating precise image-guided tumor surgery and also demonstrated the first example of liver fibrosis detection in the NIR-II window.

Furthermore, Ren *et al.* (70) reported a hybrid NIR-II fluorescent probe, a rare earth doped NP $\text{NaGdF}_4\text{:Nd}5\% @ \text{NaGdF}_4 @ \text{Lips}$ (Gd-REs@Lips), which simultaneously

performed powerful functions in both MRI and NIR-II imaging. The imaging studies on orthotopic models with xenografts established from HCC patients indicated that Gd-REs@Lips exhibited a good T2 contrast effect *in vivo*, and NIR-II fluorescence imaging detected satellite lesions on the liver surface with the smallest lesion diameter of 2 mm.

Challenges and perspectives

So far ICG and methylene blue (MB) are the only available NIR fluorophores approved by the US FDA (75). MB has not been used for regular surgical treatment due to its non-specificity and limited quantum yield. Although ICG has been reported to achieve NIR-I/II fluorescence imaging of HCC, as a non-targeted probe, ICG cannot distinguish benign and malignant tumors, and its accumulation in other tissues may lead to false positive detection of the tumor. The targeted NIRF probe needs the stable combination of the NIR fluorophore and targeting molecule to realize the fluorescence of targeted tumor cells. Once the unbound tracer is removed, the background fluorescence is expected to be significantly weakened. A variety of molecular targeted NIRF probes, recognizing vascular endothelial growth factor, carcinoembryonic antigen, EGFR and other molecular biomarkers, have been evaluated for molecular fluorescence imaging applications in the clinic (75). There is still a lack of clinical trials on HCC-targeted NIRF imaging; more importantly, no clear consensus exists on the optimal biomarkers for HCC. Molecular targets are urgently required for the early detection of HCC and the development of a novel targeted NIRF probe. Several molecular signaling pathways such as RAS-MAPK, PI3K-AKT-mTOR and WNT-TGF β , immune response related molecules such as IFN- γ , IL-4 and IL-17, tumor stem cell related molecules such as EpCAM, CD44 and CK19, tumor angiogenesis related molecules such as CXCR4, VEGFR, Prox1 and PDGF, and signal transduction related molecules such as GPC3 and integrin α 6 are involved in the development of HCC, which form a complex molecular network (76). Among them, several key molecules are expected to be promising biomarkers for HCC. For instance, GPC3, an oncofetal proteoglycan anchored to the cell membrane, is highly expressed in >70% of HCCs, but not in benign hepatic lesions, and its expression predicts a poor prognosis (77). The mechanism of GPC3 participating in HCC progression has not been fully elucidated. It is believed that GPC3 plays a role in the development of HCC by binding with Wnt signaling proteins and growth factors. Excitingly, GPC3-targeted MRI, PET and NIRF imaging

have been investigated for early HCC detection (78). With the high expression of GPC3 in the HCC cell membrane and the high tumor-to-liver ratio, we believe GPC3-targeted NIRF will have a promising future in image-guided hepatectomy of HCC. Moreover, integrin α 6, which is normally expressed on the surface of cells and consists of molecules for cell-cell and cell-extracellular matrix adhesion, has recently attracted much attention as a diagnostic marker of HCC (79). Many research groups have provided evidence of overexpression of integrin α 6 in HCC (80,81). More importantly, according to the latest report of Jiang *et al.* (82), integrin α 6 was found to be highly expressed in about 94% of early HCC. A further study reported that integrin α 6-targeted PET visualizes the small HCC lesion with a diameter of about 0.2 cm in the mouse model (83). These findings suggest that integrin α 6-targeted NIRF imaging may have a broad application prospect in the detection and resection of early HCC.

Compared with NIR-I imaging, NIR-II fluorescence imaging has significantly improved imaging performance, including real-time light detection across centimeters of tissue, micrometer resolution at depths of millimeters and high TBR, which is the future direction of optical imaging (68). As previously described, due to the limited ability of NIR-I light to penetrate human tissues, the fluorescence signals emitted by ICG can only penetrate liver parenchyma within 10 mm (36). An increasing number of proof-of-concept studies on exogenous NIR-II probes have shown that the obtained imaging penetration depth is much better than those acquired using more established contrast agents in the NIR-I window (11). However, NIR-II imaging is still difficult to break through the penetration depth of several centimeters for large parenchymal organs like the liver, and the intraoperative detection of deep HCC remains challenging. Because a deeper penetration depth can be intrinsically achieved with PA imaging and high optical absorptivity of NIR-II fluorophores can also facilitate their NIR-I or NIR-II PA imaging (11), we believe that dual-modal NIR-II fluorescence and PA imaging will be a balancing act to maximize the desired parameters for hepatectomy of HCC. Notably, Kupffer cells are specialized macrophages dispersed throughout liver sinusoids that comprise an elaborate reticuloendothelial system (RES). They take up the probes and interfere with NIRF imaging of HCC. Unfortunately, most of the existing NIR-II fluorescent probes exceed the renal filtration threshold of \approx 40 kD or \approx 5 nm hydrodynamic diameter with slow excretion and are largely retained within the RES, making clinical translation almost impossible (84). For NIR-II fluorescence imaging

applications of HCC, it is necessary to consider the timing of administration of the contrast agent and the clearance pattern of the probe. In comparison with the fluorescent agents cleared by the hepatobiliary pathway, the agents cleared by the kidneys can improve the visualization of HCC. Only a few NIR-II fluorescent agents can undergo renal clearance, which include CH1055-PEG (74), CP-IRT (84), IR-BGP6 (85), Nd-DTPA (86), Nd-DOTA (87), semiconductor CDIR2 (88), and lipoic acid-based sulfobetaine coated gold nanoclusters (89). CP-IRT MI probe was reported to possess both high tumor targeting and rapid renal excretion ($\approx 87\%$ excretion within 6 h). It was composed of a cancer stem cell marker CD133 targeting peptide CP and NIR-II emitting fluorophore IRT. While targeted imaging often relies on an antibody, the peptide has the advantages of having a small size, cell penetration, low immunogenicity, high biocompatibility, and easy synthesis. Nowadays, a variety of peptides have been found that can specifically bind to tumor biomarkers. The highly safe, NIR-II fluorescent, HCC-targeted probe composed of NIR-II agents with renal clearance ability and small molecule interface ligand is a promising strategy for HCC diagnosis and image-guided surgery.

Conclusions

During hepatic resection, reduction of normal structural damage and removal of all malignant tissue is vital for HCC patients. NIRF imaging has so far shown its high potential to support surgical procedures and the feasibility of improving clinical outcomes. Given the interest in this area, more evidence is needed to clarify the role of NIRF imaging in HCC surgery. NIR-I fluorescence imaging is rapidly progressing in hepatectomy for HCC, but there is still a lack of clinical trials of targeted probes. With the increasing number of preclinical studies, NIR-II imaging has reached a crucial turning point. In the authors' opinion, highly HCC-specific agents with fast pharmacokinetics may facilitate intraoperative HCC imaging and rapid clinical translation of the NIR-II imaging technique. It is anticipated that commercial and clinically available NIR-II fluorescent probes will be widely used in surgical resection of HCC.

Acknowledgments

The authors wish to acknowledge Karen M. von Deneen, PhD, Associate Professor, School of Life Science and Technology, Xidian University, for her help in checking the

wording of the manuscript.

Funding: This work was supported by the grants from the National Key Research and Development Program of China (2016YFC0106500, 2016YFC0102600, 2017YFA0205200), National Natural Science Foundation of China (NSFC) (81627805, 81930053, 81671759), the NSFC-GD Union Foundation, China (U1401254), National High Technology Research and Development Program of China (863 program) (2006AA02Z346, 2012AA021105), the Scientific Instrument Developing Project of the Chinese Academy of Sciences (YZ201672), Beijing Natural Science Foundation (JQ19027), Beijing Nova Program (Z181100006218046), and the innovative research team of high-level local universities in Shanghai.

Footnote

Reporting Checklist: The authors have completed the Narrative Review reporting checklist. Available at <http://dx.doi.org/10.21037/atm-20-5341>

Peer Review File: Available at <http://dx.doi.org/10.21037/atm-20-5341>

Conflicts of Interest: All authors have completed the ICMJE uniform disclosure form (available at <http://dx.doi.org/10.21037/atm-20-5341>). The authors have no conflicts of interest to declare.

Ethical Statement: The authors are accountable for all aspects of the work in ensuring that questions related to the accuracy or integrity of any part of the work are appropriately investigated and resolved.

Open Access Statement: This is an Open Access article distributed in accordance with the Creative Commons Attribution-NonCommercial-NoDerivs 4.0 International License (CC BY-NC-ND 4.0), which permits the non-commercial replication and distribution of the article with the strict proviso that no changes or edits are made and the original work is properly cited (including links to both the formal publication through the relevant DOI and the license). See: <https://creativecommons.org/licenses/by-nc-nd/4.0/>.

References

1. Villanueva A. Hepatocellular Carcinoma. *N Engl J Med* 2019;380:1450-62.

2. Forner A, Reig M, Bruix J. Hepatocellular carcinoma. *Lancet* 2018;391:1301-14.
3. Jemal A, Ward EM, Johnson CJ, et al. Annual Report to the Nation on the Status of Cancer, 1975-2014, Featuring Survival. *J Natl Cancer Inst* 2017;109:djx030.
4. Zeng H, Zheng R, Guo Y, et al. Cancer survival in China, 2003-2005: a population-based study. *Int J Cancer* 2015;136:1921-30.
5. European Association For The Study Of The Liver; European Organisation For Research And Treatment Of Cancer. EASL-EORTC clinical practice guidelines: management of hepatocellular carcinoma. *J Hepatol* 2012;56:908-43.
6. Bruix J, Sherman M. Management of hepatocellular carcinoma. *Hepatology* 2005;42:1208-36.
7. Roayaie S, Jibara G, Tabrizian P, et al. The role of hepatic resection in the treatment of hepatocellular cancer. *Hepatology* 2015;62:440-51.
8. Ishizawa T, Hasegawa K, Aoki T, et al. Neither multiple tumors nor portal hypertension are surgical contraindications for hepatocellular carcinoma. *Gastroenterology* 2008;134:1908-16.
9. Aufhauser DD, Sadot E, Murken DR, et al. Incidence of Occult Intrahepatic Metastasis in Hepatocellular Carcinoma Treated With Transplantation Corresponds to Early Recurrence Rates After Partial Hepatectomy. *Ann Surg* 2018;267:922-8.
10. Weissleder R, Pittet MJ. Imaging in the era of molecular oncology. *Nature* 2008;452:580-9.
11. Kenry, Duan Y, Liu B. Recent Advances of Optical Imaging in the Second Near-Infrared Window. *Adv Mater* 2018;30:e1802394.
12. Chance B. Near-infrared images using continuous, phase-modulated, and pulsed light with quantitation of blood and blood oxygenation. *Ann N Y Acad Sci* 1998;838:29-45.
13. Frangioni JV. In vivo near-infrared fluorescence imaging. *Curr Opin Chem Biol* 2003;7:626-34.
14. Gioux S, Choi HS, Frangioni JV. Image-guided surgery using invisible near-infrared light: fundamentals of clinical translation. *Mol Imaging* 2010;9:237-55.
15. Ishizawa T, Fukushima N, Shibahara J, et al. Real-time identification of liver cancers by using indocyanine green fluorescent imaging. *Cancer* 2009;115:2491-504.
16. Cai Y, Wei Z, Song C, et al. Optical nano-agents in the second near-infrared window for biomedical applications. *Chem Soc Rev* 2019;48:22-37.
17. Landsman ML, Kwant G, Mook GA, et al. Light-absorbing properties, stability, and spectral stabilization of indocyanine green. *J Appl Physiol* 1976;40:575-83.
18. Aoki T, Yasuda D, Shimizu Y, et al. Image-guided liver mapping using fluorescence navigation system with indocyanine green for anatomical hepatic resection. *World J Surg* 2008;32:1763-7.
19. Ishizawa T, Masuda K, Urano Y, et al. Mechanistic background and clinical applications of indocyanine green fluorescence imaging of hepatocellular carcinoma. *Ann Surg Oncol* 2014;21:440-8.
20. Gotoh K, Yamada T, Ishikawa O, et al. A novel image-guided surgery of hepatocellular carcinoma by indocyanine green fluorescence imaging navigation. *J Surg Oncol* 2009;100:75-9.
21. Satou S, Ishizawa T, Masuda K, et al. Indocyanine green fluorescent imaging for detecting extrahepatic metastasis of hepatocellular carcinoma. *J Gastroenterol* 2013;48:1136-43.
22. Morita Y, Sakaguchi T, Unno N, et al. Detection of hepatocellular carcinomas with near-infrared fluorescence imaging using indocyanine green: its usefulness and limitation. *Int J Clin Oncol* 2013;18:232-41.
23. Kudo H, Ishizawa T, Tani K, et al. Visualization of subcapsular hepatic malignancy by indocyanine-green fluorescence imaging during laparoscopic hepatectomy. *Surg Endosc* 2014;28:2504-8.
24. Zhang YM, Shi R, Hou JC, et al. Liver tumor boundaries identified intraoperatively using real-time indocyanine green fluorescence imaging. *J Cancer Res Clin Oncol* 2017;143:51-8.
25. Makuuchi M, Hasegawa H, Yamazaki S. Ultrasonically guided subsegmentectomy. *Surg Gynecol Obstet* 1985;161:346-50.
26. Aoki T, Murakami M, Yasuda D, et al. Intraoperative fluorescent imaging using indocyanine green for liver mapping and cholangiography. *J Hepatobiliary Pancreat Sci* 2010;17:590-4.
27. Ishizawa T, Zuker NB, Kokudo N, et al. Positive and negative staining of hepatic segments by use of fluorescent imaging techniques during laparoscopic hepatectomy. *Arch Surg* 2012;147:393-4.
28. Inoue Y, Arita J, Sakamoto T, et al. Anatomical Liver Resections Guided by 3-Dimensional Parenchymal Staining Using Fusion Indocyanine Green Fluorescence Imaging. *Ann Surg* 2015;262:105-11.
29. Miyata A, Ishizawa T, Tani K, et al. Reappraisal of a Dye-Staining Technique for Anatomic Hepatectomy by the Concomitant Use of Indocyanine Green Fluorescence Imaging. *J Am Coll Surg* 2015;221:e27-36.

30. Kobayashi Y, Kawaguchi Y, Kobayashi K, et al. Portal vein territory identification using indocyanine green fluorescence imaging: Technical details and short-term outcomes. *J Surg Oncol* 2017;116:921-31.
31. Sakoda M, Ueno S, Iino S, et al. Anatomical laparoscopic hepatectomy for hepatocellular carcinoma using indocyanine green fluorescence imaging. *J Laparoendosc Adv Surg Tech A* 2014;24:878-82.
32. Mizuno T, Sheth R, Yamamoto M, et al. Laparoscopic Glissonian Pedicle Transection (Takasaki) for Negative Fluorescent Counterstaining of Segment 6. *Ann Surg Oncol* 2017;24:1046-7.
33. Zhou Y, Lin Y, Jin H, et al. Real-Time Navigation Guidance Using Fusion Indocyanine Green Fluorescence Imaging in Laparoscopic Non-Anatomical Hepatectomy of Hepatocellular Carcinomas at Segments 6, 7, or 8 (with Videos). *Med Sci Monit* 2019;25:1512-7.
34. Berardi G, Wakabayashi G, Igarashi K, et al. Full Laparoscopic Anatomical Segment 8 Resection for Hepatocellular Carcinoma Using the Glissonian Approach with Indocyanine Green Dye Fluorescence. *Ann Surg Oncol* 2019;26:2577-8.
35. He JM, Zhen ZP, Ye Q, et al. Laparoscopic Anatomical Segment VII Resection for Hepatocellular Carcinoma Using the Glissonian Approach with Indocyanine Green Dye Fluorescence. *J Gastrointest Surg* 2020;24:1228-9.
36. Tanaka T, Takatsuki M, Hidaka M, et al. Is a fluorescence navigation system with indocyanine green effective enough to detect liver malignancies? *J Hepatobiliary Pancreat Sci* 2014;21:199-204.
37. Vahrmeijer AL, Hutteman M, van der Vorst JR, et al. Image-guided cancer surgery using near-infrared fluorescence. *Nat Rev Clin Oncol* 2013;10:507-18.
38. Schneider AR, Zöpf T, Arnold JC, et al. Feasibility and diagnostic impact of fluorescence-based diagnostic laparoscopy in hepatocellular carcinoma: a case report. *Endoscopy* 2002;34:831-4.
39. Inoue Y, Tanaka R, Komeda K, et al. Fluorescence detection of malignant liver tumors using 5-aminolevulinic acid-mediated photodynamic diagnosis: principles, technique, and clinical experience. *World J Surg* 2014;38:1786-94.
40. Kaibori M, Matsui K, Ishizaki M, et al. Intraoperative Detection of Superficial Liver Tumors by Fluorescence Imaging Using Indocyanine Green and 5-aminolevulinic Acid. *Anticancer Res* 2016;36:1841-9.
41. Chung IW, Eljamel S. Risk factors for developing oral 5-aminolevulinic acid-induced side effects in patients undergoing fluorescence guided resection. *Photodiagnosis Photodyn Ther* 2013;10:362-7.
42. Hu Z, Chen WH, Tian J, et al. NIRF Nanoprobes for Cancer Molecular Imaging: Approaching Clinic. *Trends Mol Med* 2020;26:469-82.
43. Li FQ, Zhang SX, An LX, et al. In vivo molecular targeting effects of anti-Sp17- ICG-Der-02 on hepatocellular carcinoma evaluated by an optical imaging system. *J Exp Clin Cancer Res* 2011;30:25.
44. Lv F, He X, Wu L, et al. Lactose substituted zinc phthalocyanine: a near infrared fluorescence imaging probe for liver cancer targeting. *Bioorg Med Chem Lett* 2013;23:1878-82.
45. He H, Tu X, Zhang J, et al. A novel antibody targeting CD24 and hepatocellular carcinoma in vivo by near-infrared fluorescence imaging. *Immunobiology* 2015;220:1328-36.
46. Zhu D, Qin Y, Wang J, et al. Novel Glypican-3-Binding Peptide for in Vivo Hepatocellular Carcinoma Fluorescent Imaging. *Bioconj Chem* 2016;27:831-9.
47. Qin Z, Wang J, Wang Y, et al. Identification of a Glypican-3-Binding Peptide for In Vivo Non-Invasive Human Hepatocellular Carcinoma Detection. *Macromol Biosci* 2017. doi: 10.1002/mabi.201600335.
48. Zeng C, Shang W, Wang K, et al. Intraoperative Identification of Liver Cancer Microfoci Using a Targeted Near-Infrared Fluorescent Probe for Imaging-Guided Surgery. *Sci Rep* 2016;6:21959.
49. Li Z, Zhou Q, Zhou J, et al. In vivo fluorescence imaging of hepatocellular carcinoma xenograft using near-infrared labeled epidermal growth factor receptor (EGFR) peptide. *Biomed Opt Express* 2016;7:3163-9.
50. An J, Zhao N, Zhang C, et al. Heptamethine carbocyanine DZ-1 dye for near-infrared fluorescence imaging of hepatocellular carcinoma. *Oncotarget* 2017;8:56880-92.
51. Tang C, Du Y, Liang Q, et al. Development of a Novel Histone Deacetylase-Targeted Near-Infrared Probe for Hepatocellular Carcinoma Imaging and Fluorescence Image-Guided Surgery. *Mol Imaging Biol* 2020;22:476-85.
52. Liu Y, Feng B, Cao X, et al. A novel "AIE + ESIPT" near-infrared nanoprobe for the imaging of γ -glutamyl transpeptidase in living cells and the application in precision medicine. *Analyst* 2019;144:5136-42.
53. Wu L, Ishigaki Y, Hu Y, et al. HS-activatable near-infrared afterglow luminescent probes for sensitive molecular imaging in vivo. *Nat Commun* 2020;11:446.
54. Park JO, Stephen Z, Sun C, et al. Glypican-3 targeting of liver cancer cells using multifunctional nanoparticles. *Mol*

- Imaging 2011;10:69-77.
55. Liu J, Li Z, Yang X, et al. A high-performance imaging probe with NIR luminescence and synergistically enhanced T1-T2 relaxivity for in vivo hepatic tumor targeting and multimodal imaging. *Chem Commun (Camb)* 2015;51:13369-72.
 56. Hernandez R, Sun H, England CG, et al. CD146-targeted immunoPET and NIRF Imaging of Hepatocellular Carcinoma with a Dual-Labeled Monoclonal Antibody. *Theranostics* 2016;6:1918-33.
 57. Chen Q, Shang W, Zeng C, et al. Theranostic imaging of liver cancer using targeted optical/MRI dual-modal probes. *Oncotarget* 2017;8:32741-51.
 58. Guan T, Shang W, Li H, et al. From Detection to Resection: Photoacoustic Tomography and Surgery Guidance with Indocyanine Green Loaded Gold Nanorod@liposome Core-Shell Nanoparticles in Liver Cancer. *Bioconjug Chem* 2017;28:1221-8.
 59. Yan H, Gao X, Zhang Y, et al. Imaging Tiny Hepatic Tumor Xenografts via Endoglin-Targeted Paramagnetic/Optical Nanoprobe. *ACS Appl Mater Interfaces* 2018;10:17047-57.
 60. Jin Y, Wang K, Tian J. Preoperative Examination and Intraoperative Identification of Hepatocellular Carcinoma Using a Targeted Bimodal Imaging Probe. *Bioconjug Chem* 2018;29:1475-84.
 61. Zhang C, Zhao Y, Zhao N, et al. NIRF Optical/PET Dual-Modal Imaging of Hepatocellular Carcinoma Using Heptamethine Carbocyanine Dye. *Contrast Media Mol Imaging* 2018;2018:4979746.
 62. Ai T, Shang W, Yan H, et al. Near infrared-emitting persistent luminescent nanoparticles for Hepatocellular Carcinoma imaging and luminescence-guided surgery. *Biomaterials* 2018;167:216-25.
 63. Shuai T, Zhou Y, Shao G, et al. Bimodal Molecule as NIR-CT Contrast Agent for Hepatoma Specific Imaging. *Anal Chem* 2020;92:1138-46.
 64. Nappi C, Altiero M, Imbriaco M, et al. First experience of simultaneous PET/MRI for the early detection of cardiac involvement in patients with Anderson-Fabry disease. *Eur J Nucl Med Mol Imaging* 2015;42:1025-31.
 65. Omata M, Cheng AL, Kokudo N, et al. Asia-Pacific clinical practice guidelines on the management of hepatocellular carcinoma: a 2017 update. *Hepatol Int* 2017;11:317-70.
 66. Schraml C, Kaufmann S, Rempp H, et al. Imaging of HCC-Current State of the Art. *Diagnostics (Basel)* 2015;5:513-45.
 67. Wang LV, Hu S. Photoacoustic tomography: in vivo imaging from organelles to organs. *Science* 2012;335:1458-62.
 68. Hu Z, Fang C, Li B, et al. First-in-human liver-tumour surgery guided by multispectral fluorescence imaging in the visible and near-infrared-I/II windows. *Nat Biomed Eng* 2020;4:259-71.
 69. Ding F, Li C, Xu Y, et al. PEGylation Regulates Self-Assembled Small-Molecule Dye-Based Probes from Single Molecule to Nanoparticle Size for Multifunctional NIR-II Bioimaging. *Adv Healthc Mater* 2018;7:e1800973.
 70. Ren Y, He S, Huttad L, et al. NIR-II/MR Dual Modal Nanoprobe for Liver Cancer Imaging. *Nanoscale* 2020;12:11510-7.
 71. He S, Song J, Qu J, et al. Crucial breakthrough of second near-infrared biological window fluorophores: design and synthesis toward multimodal imaging and theranostics. *Chem Soc Rev* 2018;47:4258-78.
 72. Antaris AL, Chen H, Diao S, et al. A high quantum yield molecule-protein complex fluorophore for near-infrared II imaging. *Nat Commun* 2017;8:15269.
 73. Carr JA, Franke D, Caram JR, et al. Shortwave infrared fluorescence imaging with the clinically approved near-infrared dye indocyanine green. *Proc Natl Acad Sci U S A* 2018;115:4465-70.
 74. Antaris AL, Chen H, Cheng K, et al. A small-molecule dye for NIR-II imaging. *Nat Mater* 2016;15:235-42.
 75. Hernot S, van Manen L, Debie P, et al. Latest developments in molecular tracers for fluorescence image-guided cancer surgery. *Lancet Oncol* 2019;20:e354-e367.
 76. Zucman-Rossi J, Villanueva A, Nault JC, et al. Genetic Landscape and Biomarkers of Hepatocellular Carcinoma. *Gastroenterology* 2015;149:1226-1239.e4.
 77. Capurro M, Wanless IR, Sherman M, et al. Glypican-3: a novel serum and histochemical marker for hepatocellular carcinoma. *Gastroenterology* 2003;125:89-97.
 78. Zhou F, Shang W, Yu X, et al. Glypican-3: A promising biomarker for hepatocellular carcinoma diagnosis and treatment. *Med Res Rev* 2018;38:741-67.
 79. Hood JD, Cheresch DA. Role of integrins in cell invasion and migration. *Nat Rev Cancer* 2002;2:91-100.
 80. Bergamini C, Sgarra C, Trerotoli P, et al. Laminin-5 stimulates hepatocellular carcinoma growth through a different function of alpha6beta4 and alpha3beta1 integrins. *Hepatology* 2007;46:1801-9.
 81. Kim YR, Byun MR, Choi JW. Integrin $\alpha 6$ as an invasiveness marker for hepatitis B viral X-driven hepatocellular carcinoma. *Cancer Biomark* 2018;23:135-44.

82. Jiang Y, Sun A, Zhao Y, et al. Proteomics identifies new therapeutic targets of early-stage hepatocellular carcinoma. *Nature* 2019;567:257-61.
83. Feng GK, Ye JC, Zhang WG, et al. Integrin $\alpha 6$ targeted positron emission tomography imaging of hepatocellular carcinoma in mouse models. *J Control Release* 2019;310:11-21.
84. Wang W, Ma Z, Zhu S, et al. Molecular Cancer Imaging in the Second Near-Infrared Window Using a Renal-Excreted NIR-II Fluorophore-Peptide Probe. *Adv Mater* 2018;30:e1800106.
85. Wan H, Ma H, Zhu S, et al. Developing a Bright NIR-II Fluorophore with Fast Renal Excretion and Its Application in Molecular Imaging of Immune Checkpoint PD-L1. *Adv Funct Mater* 2018;28:1804956.
86. Li Y, Li X, Xue Z, et al. Second near-infrared emissive lanthanide complex for fast renal-clearable in vivo optical bioimaging and tiny tumor detection. *Biomaterials* 2018;169:35-44.
87. Yang Y, Wang P, Lu L, et al. Small-Molecule Lanthanide Complexes Probe for Second Near-Infrared Window Bioimaging. *Anal Chem* 2018;90:7946-52.
88. Huang J, Xie C, Zhang X, et al. Renal-clearable Molecular Semiconductor for Second Near-Infrared Fluorescence Imaging of Kidney Dysfunction. *Angew Chem Int Ed Engl* 2019;58:15120-7.
89. Chen Y, Montana DM, Wei H, et al. Shortwave Infrared in Vivo Imaging with Gold Nanoclusters. *Nano Lett* 2017;17:6330-4.

Cite this article as: Zhang W, Hu Z, Tian J, Fang C. A narrative review of near-infrared fluorescence imaging in hepatectomy for hepatocellular carcinoma. *Ann Transl Med* 2021;9(2):171. doi: 10.21037/atm-20-5341